Mapping of ice layer extent and snow accumulation in the percolation zone of the Greenland ice sheet

S. V. Nghiem,[1] K. Steffen,[2] G. Neumann,[1] and R. Huff[2]

Received 5 September 2004; revised 11 March 2005; accepted 13 April 2005; published 25 June 2005.

[1] The Greenland ice sheet underwent record extensive melt in 2002 and prolonged melt in 2003. The severe melting created a significant and extensive ice layer over the Greenland ice sheet. An innovative approach is developed to detect the ice layer formation using data acquired by the SeaWinds scatterometer on the QuikSCAT satellite. QuikSCAT backscatter together with in situ data from automatic weather stations of the Greenland Climate Network are used to map the extent of ice layer formation. The results reveal areas of extensive ice layer formed by the 2002 melt, which is consistent with the maximum melt extent in 2002. Moreover, during freezing seasons, QuikSCAT data show a linear decrease in backscatter (in decibels or dB) that is related to the amount of snow accumulation in the ice layer formation region. This snow accumulation signature is caused by the attenuation of radar waves in the snow layer, accumulating since the last major melt event, whose thickness appears as an exponential function in relation to the backscatter signature. We use the Greenland Climate Network data to calibrate the QuikSCAT accumulation rate in order to estimate and map snow accumulation. QuikSCAT results capture the extreme snowfall in mid-April 2003, which deposited more than 0.5 m of snow in a day as measured by the automated weather station at the NASA South East site. Large-scale QuikSCAT results show an anomalous increase of snow accumulation over the southeast region of Greenland during the 2002–2003 freezing season.

Citation: Nghiem, S. V., K. Steffen, G. Neumann, and R. Huff (2005), Mapping of ice layer extent and snow accumulation in the percolation zone of the Greenland ice sheet, *J. Geophys. Res.*, *110*, F02017, doi:10.1029/2004JF000234.

1. Introduction

[2] In light of possible future sea level rise, a pressing need exists for precise knowledge of the mass balance of large ice sheets like Antarctica and Greenland. The deposition and accumulation of water as snow on the ice sheet are key components of mass balance. Changes in ice sheet thickness with time have been inferred from aircraft [*Krabill et al.*, 2004; *Thomas et al.*, 2003] and satellite data [*Zwally et al.*, 1998; *Davis et al.*, 1998]. The Greenland ice sheet shows little change in overall mass, although significant thinning has been found near coastal regions particularly in the western part of Greenland.

[3] The first satellite-borne radar remote sensing systems, including an L-band synthetic aperture radar (SAR) and a Ku-band scatterometer, were flown on the Seasat satellite in 1978. The SAR provided high-resolution images, but only over a narrow swath with limited spatial and temporal sampling. Nevertheless, it has been a useful tool for studying polar ice [*Jezek et al.*, 1993]. Studies of Greenland and Antarctica ice sheets take advantage of the sensitivity of backscatter to the density and grain size in the various ice facies, especially in the percolation zone and during summer melt. This approach provides a means of examining long-term variability over the ice sheets, particularly, including the extent of the seasonal snowmelt zone over Greenland [*Wismann*, 2000; *Smith et al.*, 2003]. Estimates of changes in accumulation rates over ice sheets have been made over Greenland [*Drinkwater et al.*, 2001] using scatterometer data from multiple sensors.

[4] With the launch of ICESat (Ice, Cloud, and land Elevation Satellite Mission), a new tool became available to map surface height changes of the ice sheet from space. In the ablation region, height changes can be related to surface melt and to the dynamic response of the ice sheet (e.g., dynamic thinning in the Jakobshavn region [*Thomas et al.*, 2003]). In the dry snow region, height changes are related to changes in snow accumulation and variations in firn density [*Zwally and Jun*, 2002]. In the remaining part of the ice sheet, the percolation zone (more than 1/3 of the ice sheet area), the surface height change is the result of spatial and temporal variability in snow accumulation [*McConnell et al.*, 2000] and variations in near-surface firn density [*Braithwaite et al.*, 1994].

[1] Jet Propulsion Laboratory, California Institute of Technology, Pasadena, California, USA.
[2] Cooperative Institute for Research in Environmental Sciences, University of Colorado, Boulder, Colorado, USA.

0148-0227/05/2004JF000234$09.00

[5] The maximum melt extent of the Greenland ice sheet has increased approximately 16% from 1979 to 2002 on the basis of passive microwave (PM) satellite data [*Steffen et al.*, 2004]. The total area of surface melt on the Greenland ice sheet broke all known records for the island in summer 2002, with a melt area of 690,000 km^2 significantly exceeding an average melt extent of 455,000 km^2 from 1979 to 2003 observed by PM data [*Steffen et al.*, 2004]. With increased melt in the percolation region, the snow and firn layers increase in density because of the percolation and refreezing of meltwater, reducing the surface height by near-surface densification. Thus information on the melt densification is important to accurately estimate ice mass balance.

[6] In this paper, we present (1) the first method to map the extent of ice layer formation where densification is significant because of summer melt and (2) a new method to map snow accumulation in the percolation zone using QuikSCAT data. The Greenland Climate Network data are important in both algorithm development and result verification. We show the first maps of the ice layer extent caused by the record summer melt in 2002 and of anomalous snow accumulation is in southeast Greenland during the 2002–2003 freezing season.

2. Greenland Climate Network

[7] We use in situ data measured by the Greenland Climate Network (GC-Net) for the interpretation of QuikSCAT signatures to develop algorithms to detect and map the extent of ice layer formation and snow accumulation. The GC-Net was established in spring 1995 with the intention of monitoring climatological and glaciological parameters at various locations on the ice sheet over a time period of at least 15 years [*Steffen and Box*, 2001]. GC-Net currently consists of 18 automatic weather stations distributed over the entire Greenland ice sheet (Figure 1). Four stations are located along the crest of the ice sheet (2500 to 3200 m elevation range) in a north-south direction, eight stations are located close to the 2000 m contour line (1830 m to 2500 m), four stations are positioned in the ablation region (50 m to 800 m), and two stations are located at the equilibrium line altitude on the west coast and in the northwest.

[8] The objectives of the GC-Net stations are to measure hourly, daily, annual and interannual variability in accumulation rate, surface climatology and surface energy balance parameters at selected locations on the ice sheet, and to monitor near-surface snow temperatures at the automated weather station (AWS) locations for the assessment of snow densification, accumulation, and metamorphosis. Each AWS is equipped with a number of meteorological instruments (Figure 1) to measure the following parameters: (1) the surface height change at high temporal resolution to identify and resolve individual precipitation events and storms, (2) the radiation balance at the surface, (3) temperature, humidity and wind speed profiles in the surface boundary layer, and (4) the snowpack conductive heat flux that also describes the energy dissipation from refreezing of percolated meltwater. Additional meteorological parameters such as wind direction, pressure, and short-wave incoming and reflected radiation are also recorded.

3. Timing of Melt and Freezing

3.1. QuikSCAT Data for Melt Monitoring

[9] During snowmelt and refreezing processes, snow metamorphoses and backscatter signatures are complicated. The timing of melt and refreezing is important for mapping ice layer formation extent and snow accumulation, which requires stable backscatter data in freezing seasons. We have developed a method to accurately determine timing of melt and freezing from QuikSCAT data and verify results with GC-Net data [*Nghiem et al.*, 2001]. QuikSCAT is suitable for this application because it is able to monitor changes on diurnal as well as seasonal timescales over a large area. The QuikSCAT satellite was launched in June 1999, and carries a SeaWinds scatterometer (Ku-band, 13.4 GHz) accurately measuring global backscatter ($\sim$0.2 dB accuracy) with a swath of 1800 km for the vertical (V) polarization and 1400 km for the horizontal (H) polarization [*Tsai et al.*, 2000]. QuikSCAT completely covers Greenland two times per day (around local 6:20 am and pm). We use the vertical polarization cell data with an approximate spatial resolution of 25 km $\times$ 25 km for melt mapping.

3.2. QuikSCAT Melt Signature

[10] As an example, we show more than 4 years of QuikSCAT and AWS data at the NASA South East (NASA-SE) station in Figure 2. This station is located in the percolation zone of the southeastern region of Greenland at 66.48°N and 42.5°W (Figure 1). When the surface snow layer undergoes melting, backscatter drops significantly as seen in Figure 2a. The QuikSCAT diurnal signature is defined as the difference between morning and evening backscatter (in dB, commonly used in radar remote sensing). It is 10 times the base-10 logarithm of the number proportional to the ratio of morning backscatter over evening backscatter. The diurnal signal can change significantly and can take on both positive and negative values as shown in the second panel in Figure 3b. In situ temperature measured at the NASA-SE AWS in Figure 2c verifies the melting conditions detected by QuikSCAT. Our melt detection algorithm uses the diurnal difference in the backscatter signature between day and night. Detail of the algorithm is published by *Nghiem et al.* [2001]. This approach does not depend on absolute backscatter and is independent of the long-term drift of the radar gain. This allows a consistent interannual monitoring of melt regions, while the high temporal resolution allows observations of melt events on the daily timescale.

3.3. Melt/Freeze Timing From QuikSCAT

[11] Dates for the first and the last melt mark the melt time blocks in 1999–2003 as presented in Figure 2 and listed in Table 1. For our purpose, we define the melt time block, $\Delta\tau_m$, as the time between the first and the last melt, in which melt events can occur intermittently with multiple melt and refreezing cycles. Results reveal large interannual variability in the first- and the last-melt date, and in the melt time block $\Delta\tau_m$. Note that a longer $\Delta\tau_m$ does not necessarily

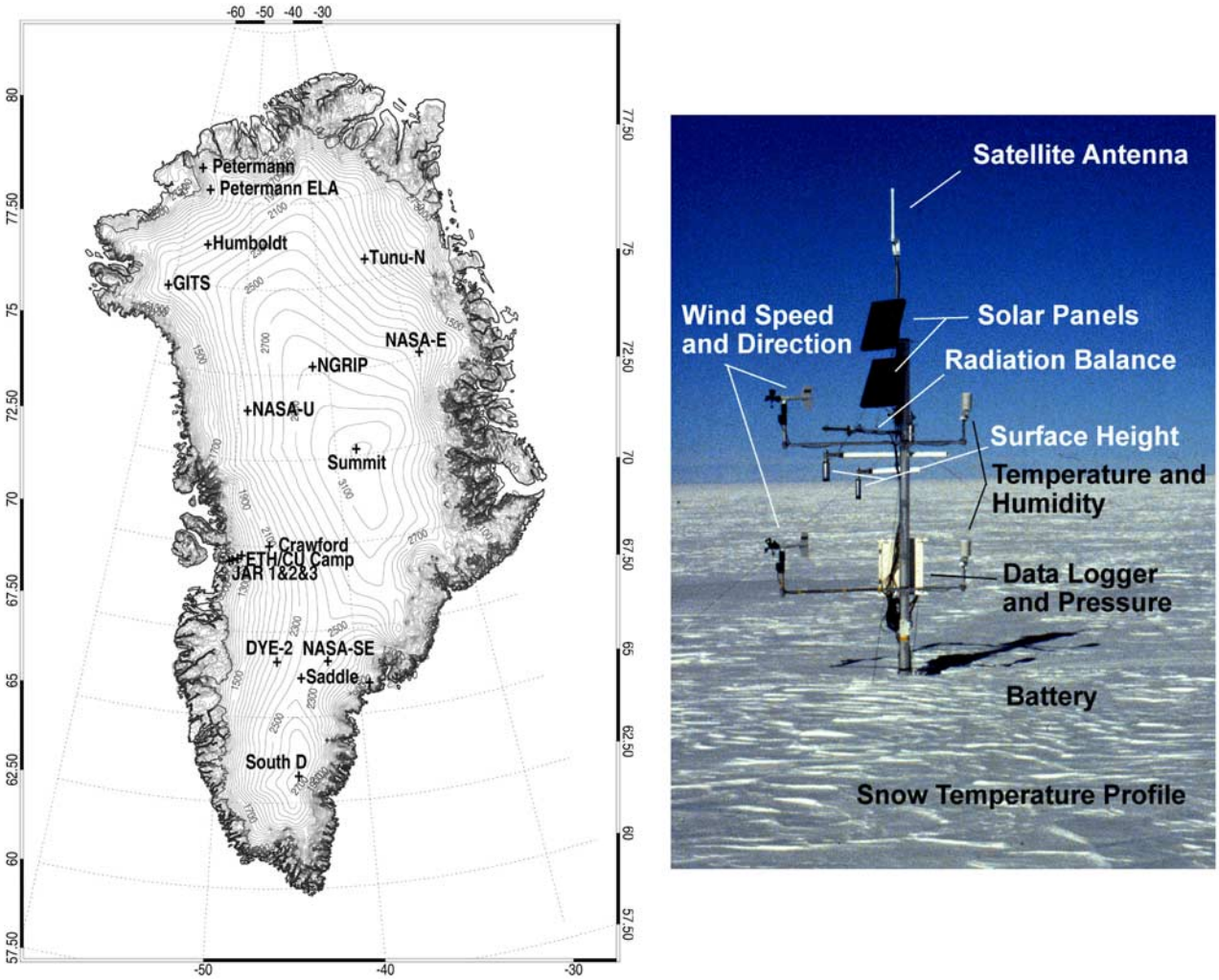

Figure 1. (left) Location map of the Greenland Climate Network (GC-Net) automatic weather stations (AWS). (right) Humboldt AWS with instruments. The 4 × 100 Ah batteries are buried beneath the AWS tower in a wood box, and the snow temperatures are measured with a 10-m thermocouple string extending from the data logger box. More information about the GC-Net is given by *Steffen and Box* [2001].

mean stronger melt or a larger number of melt days within $\Delta\tau_m$, and there can be periods of no melt (intermittent refreezing periods) in $\Delta\tau_m$. We define $\Delta\tau_m$ in this manner for the specific application of ice layer formation and snow accumulation mapping to be described later. Both melt timing and $\Delta\tau_m$ vary spatially in the percolation zone. Within a melt time block $\Delta\tau_m$, absolute backscatter is complex and varies significantly (see Figure 2).

[12] We define a freezing season as the time duration between two consecutive melt time blocks $\Delta\tau_m$ (not just between two isolated melt events). As defined, a freezing season lasts several months and contains no detectable melt event (Figure 2). We use the term freezing "season" to be consistent with the seasonal timescale (several months), and to distinguish with an intermittent refreezing "period" on timescales of days to weeks within a melt time block $\Delta\tau_m$ (Figure 2). During a freezing season, backscatter is very stable and can be used to detect the ice layer formed during the preceding melt time block and to estimate total snow accumulation. Therefore the first step is to determine the timing of the first and last melt, extract $\Delta\tau_m$, and select the freezing season for stable backscatter.

4. Detection of Extent of Ice Layer Formation

4.1. QuikSCAT Signature of Ice Layer Formation

[13] The ice layer formation extent is defined as the spatial extent of an ice layer formed during a melt time block. An ice layer consists of bigger scatterers such as clumps of coalesced ice grains, icicles, ice columns, or ice lenses formed by the percolation of melting water (Figure 3) that refreezes in the firn layer. Once created, the ice layer remains in place during the subsequent freezing season and becomes buried as snow accumulates. Large scatterers in the ice layer can dominate radar backscatter. In fact, from surface-based C-band radar measurements at a site on the western flank of Greenland, *Jezek et al.* [1993] identified

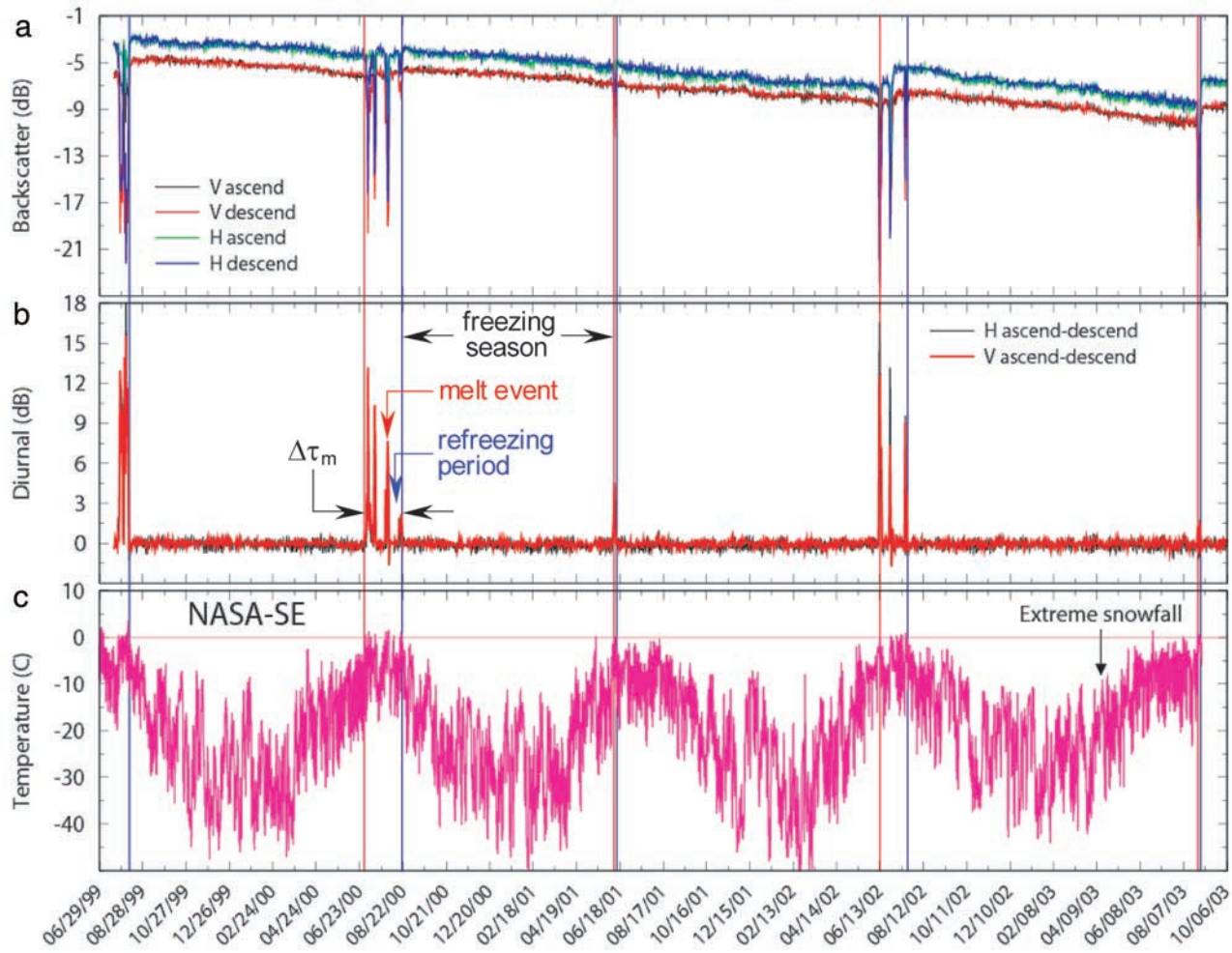

Figure 2. Time series (more than 4 years) for the NASA-SE site. (a) QuikSCAT backscatter, (b) QuikSCAT diurnal signatures, and (c) AWS air temperature. Vertical red/blue lines are for first- and last-melt dates, respectively. The arrow indicates the date (15 April 2003) when an extreme snowfall occurred while the temperature was well below freezing.

strong backscatter from summer ice lenses formed within the previous winter's snowpack.

[14] Results in Figure 2 show Ku-band backscatter response before and after four different melt time blocks in 2000–2003 at the NASA-SE location. Clear jumps in horizontally polarized backscatter of 1.5 dB in 2002 and 2.0 dB in 2003 (46° incidence angle) indicate the formation of ice layers containing large ice scatterers. Backscatter with the vertical polarization (54° incidence angles) also shows the jumps in 2002 and 2003 with weaker changes in amplitude compared to those with the horizontal polarization. Given the scatterometer measurement accuracy of about 0.2 dB (3σ) [*Tsai et al.*, 2000], these backscatter jumps are well above the signal accuracy limit. No significant increase in backscatter was observed across the 2001 melt time block indicating little or no new ice layer formation. Hence the backscatter from ice layers formed in previous years is still the main source of the signal. Figure 3 shows the ice layer formed during the 2002 melt time block and the corresponding QuikSCAT backscatter increase of 4.4 dB at the NASA East (NASA-E) location. Field measurements at this location confirm a 2-cm thick ice layer and a number of vertical percolation features at the 2002 summer horizon in the snowpack.

4.2. QuikSCAT Algorithm for Detection of Ice Layer Formation

[15] The approach is to subtract the biweekly averaged backscatter before and after a melt time block to determine the backscatter change in the dB domain. The new extent of the ice layer formed in a given year is detected on the basis of the backscatter increase after the $\Delta\tau_m$ in the corresponding year. We take a backscatter increase of 0.5 dB or more after the last-melt day as a result of the formation of ice scatterers in the snow layer. We select the backscatter increase value of 0.5 dB (2.5 times of the QuikSCAT measurement accuracy) to ensure the change is significantly above the uncertainty of 0.2 dB in each of the two backscatter values before and after $\Delta\tau_m$. This is because a lower value of the backscatter increase would contain a larger uncertainty while a higher value might underestimate the area of the ice layer formation. This algorithm, using analysis in the time domain, demands that each pixel is treated not as a single point measure-

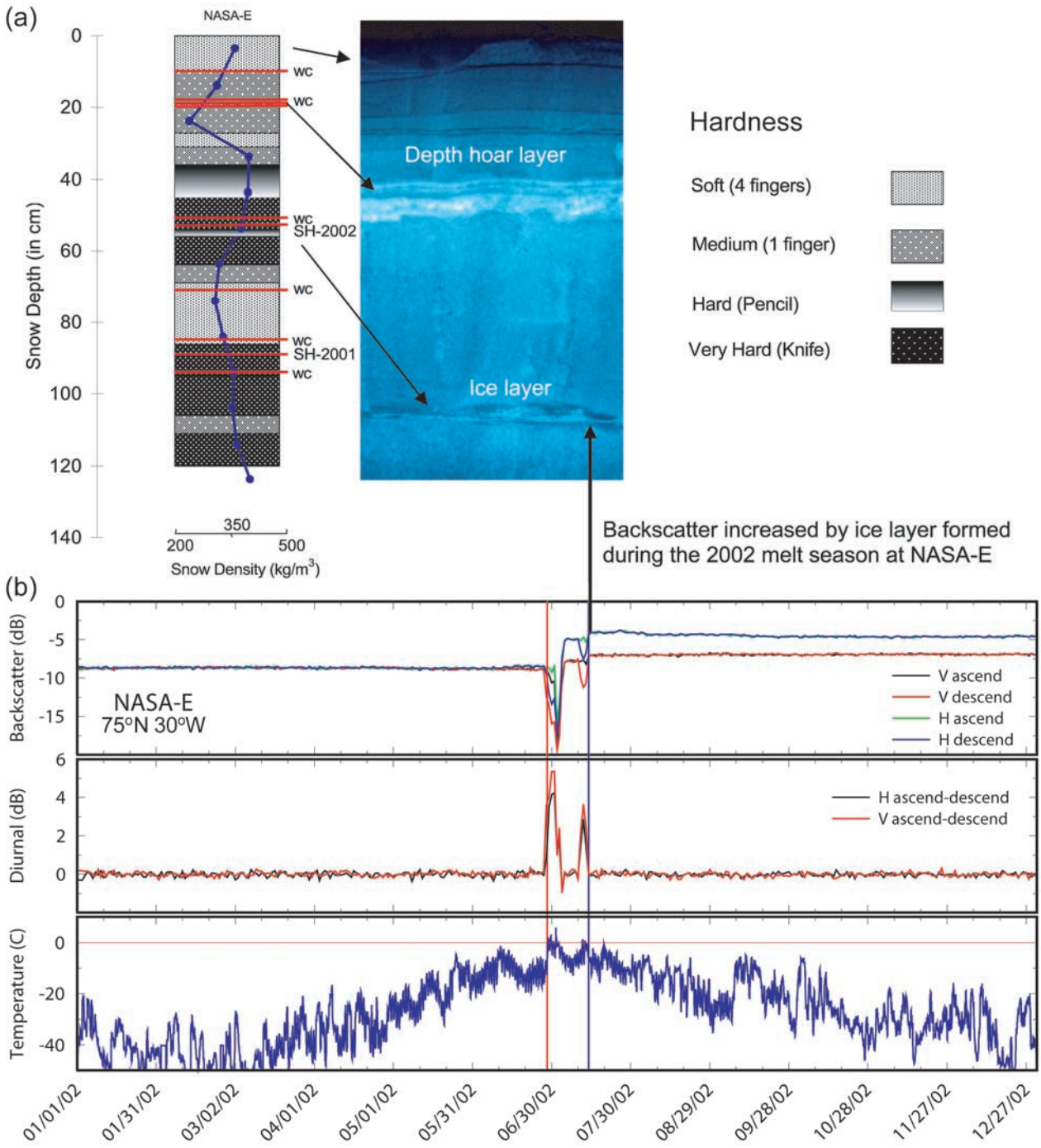

Figure 3. (a) Stratigraphy of snow pit depicting several wind crusts (WC), a 2-cm thick ice layer, and a distinct depth hoar layer at NASA-E location. The hardness for each layer is provided by a gray scale and is explained to the right of the graph. (b) Plots of QuikSCAT signatures at NASA-E showing the 2002 melt time block from the first-melt date (red vertical line on the three graphs) to the last-melt date (blue vertical line) and the backscatter increased by the ice layer formation in 2002.

ment but rather as a time series record such as those shown in Figures 2 and 3.

4.3. Mapping Extent of Ice Layer Formation

[16] The ice layer formation map in Figure 4, derived from QuikSCAT horizontal polarization cell data, reveals extensive ice formation over the Greenland ice sheet in 2002. The area outside the black contour in Figure 4 is the passive microwave–derived melt area, which is the most extensive from the passive microwave data record in the past 25 years [*Sturm et al.*, 2003; *Steffen et al.*, 2004]. On the ice layer formation map in Figure 4, we

Table 1. First-Melt Dates, Last-Melt Dates, and Melt Time Block $\Delta\tau_m$ in 1999–2003 at NASA-SE[a]

	1999	2000	2001	2002	2003
First-melt date	na	30 June	10 June	13 June	27 August
Last-melt date	6 August	21 August	14 June	20 July	31 August
$\Delta\tau_m$	na	53 days	5 days	38 days	5 days

[a]Abbreviation na is not applicable.

also overlaid the blue contour representing the melt extent (two or more days) detected by QuikSCAT. The difference between the passive microwave– and the QuikSCAT-derived melt areas is explained in detail by *Steffen et al.* [2004]. The band of ice layer formation along the southeast, south, and southwest areas in the Greenland percolation zone was mostly confined within the passive microwave melt extent, which signifies a later or stronger melt compared to the QuikSCAT melt result [*Steffen et al.*, 2004].

[17] All of the 2002 ice layer formation was within the QuikSCAT melt extent; however, there are QuikSCAT melt areas with no detectable ice layers. This could be due to early or weak melt in these areas, or due to snow accumulation that melted into an ice layer from a previous year (e.g., west flank of the Greenland ice sheet). In western Greenland, the area of ice layer formation coincides with the region from the higher-elevation side of the passive microwave melt area to the boundary of the QuikSCAT melt contour, located well into the dry snow zone. This anomalously extensive ice layer formation was created during the 2002 melt season, which itself was extensive. Similar anomalously extensive areas of ice layer formation occurred on the north and east sides of the Greenland ice sheet (Figure 4). A map of melting days derived from QuikSCAT is shown for comparison (Figure 5). Figure 5 indicates that ice layer formation can occur in areas experiencing as few as two days of melt. Furthermore, the ice layer formation map (Figure 4) shows that the major portion of the ice formation is within the percolation zone of the Greenland ice sheet defined by *Benson* [1962] (Figure 5); however, because of the 2002 record melt, the ice layer formation extends well into the dry snow zone defined by Benson.

[18] Regions of the 2002 ice layer formation (Figure 4) were obtained by subtracting biweekly averaged backscatter values between 23 March and 7 October 2002, to ensure that the 2002 $\Delta\tau_m$ was fully enclosed. Consequently, some regions of ice layer formation might be missing because of differences in melting and attenuation by snow accumulation in different regions of Greenland. Thus the ice layer formation extent shown in Figure 4 is a conservative measure of the true extent. Quantitative knowledge of ice layer formation and extent is crucial in a changing climate because a change in surface density causes an elevation change without a corresponding change in accumulation. Ice sheet elevation change derived from aircraft (laser altimeter repeat survey) or satellite (ICESat, or the forthcoming CryoSat) is not only a response to accumulation change but is also due to differential snow densification. Given the increase in the aerial extent of melt on the Greenland ice sheet, in particular during the last decade, changes in snow density (e.g., due to an increase in the number of ice layers) can account for surface elevation changes as observed in the southwestern region of the ice sheet.

5. Estimation of Snow Accumulation

5.1. QuikSCAT Signature of Snow Accumulation

[19] Several methods have been used to estimate snow accumulation (SA) over the Greenland ice sheet. C-band ERS-1 SAR data in September–November 1992 were used to estimate snow accumulation in the dry snow zone of the Greenland ice sheet [*Munk et al.*, 2003]. C-band ERS

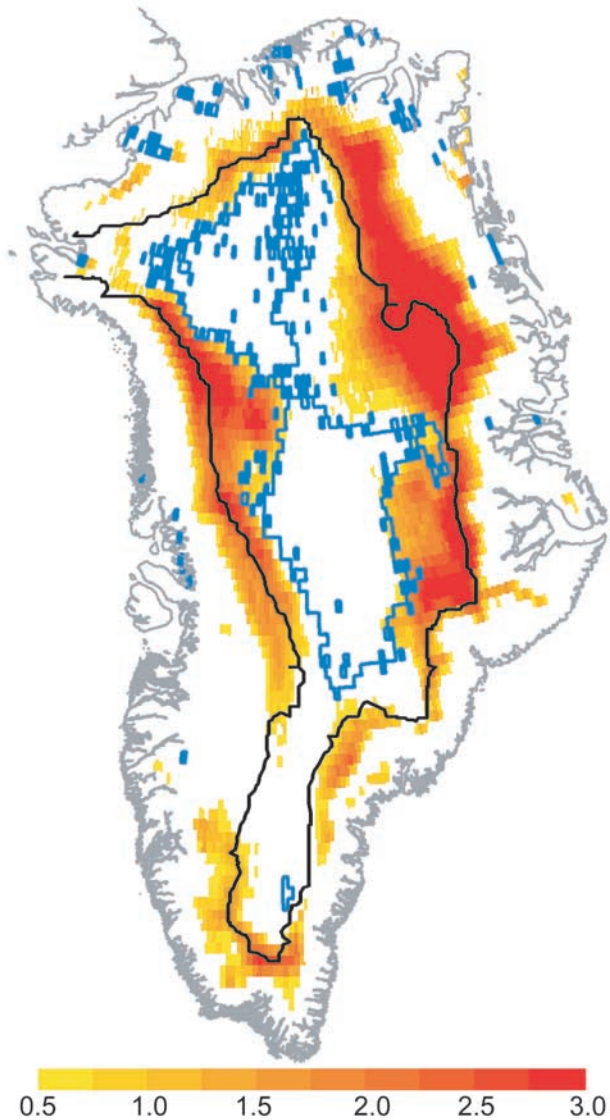

Figure 4. Extent of ice layer formation overlaid with the backscatter difference (color scale unit in dB) derived from QuikSCAT data between 7 October 2002 (after the last melt) and 23 March 2002 (before the first melt). The region outside the black contour is the maximum melt area extent derived from passive microwave data. The region outside the blue contour is the melt extent where two or more melt days were observed by QuikSCAT.

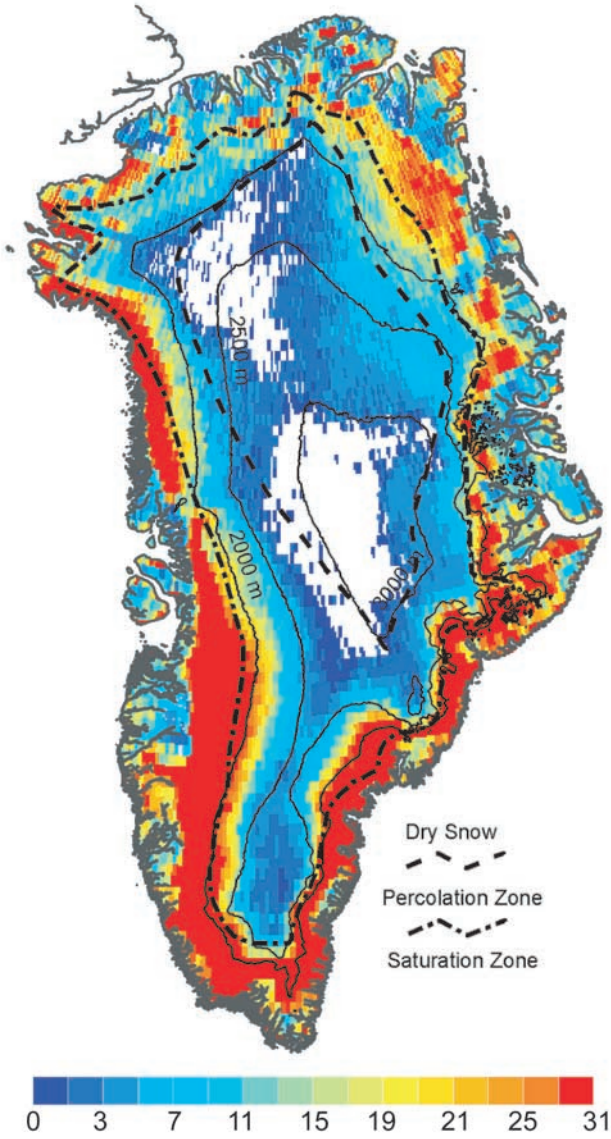

Figure 5. Number of melt days as derived from QuikSCAT in 2002 (color scale unit in days). Solid line contours represent the pattern of the Greenland topography. Benson's facies [*Benson*, 1962] including dry snow, percolation, and saturation zones are delineated by the dashed and dash-dotted contours.

scatterometer and Ku-band NSCAT scatterometer data were also used. ERS scatterometer data are collected with a small single-sided swath with a coarse resolution of 50 km. The NSCAT data set is better in terms of swath width and resolution, but the mission lasted only 9 months. *Drinkwater et al.* [2001] used backscatter slope obtained from the NASA Scatterometer (NSCAT) data with multi-incidence angles to estimate SA. Unlike NSCAT, QuikSCAT does not have multiple incidence angles, but only a single incidence angle for each different polarization beam, hence the NSCAT approach is not applicable. We present a new method to retrieve snow accumulation depth from QuikSCAT data on a daily to weekly basis for the percolation regions of the Greenland ice sheet.

[20] As snow accumulates, the backscatter contribution from the ice layer, consisting of large scatterers (Figure 3) created by melt metamorphosis of firn layers, becomes weaker because of the two-way attenuation (incoming and backscattering paths) in the snow. Thus snow attenuation forces the backscatter to decrease during freezing seasons as seen in Figure 2. The multiyear backscatter signatures at the NASA-SE (Figure 6) depict in detail the backscatter decrease during 1999–2003 freezing seasons together with snow accumulation depth (above the snow level on 1/1/1999) at NASA-SE AWS. We observe several interesting features in Figure 6: (1) the linearity in both backscatter decrease and in snow accumulation, (2) an anomalously high snow accumulation rate and total snow accumulation during most of the 2002–2003 freezing season, (3) several sharp increases in accumulation including an extreme snowfall in the middle of April 2003, and (4) lowering of snow surface height after the extraordinary snow event in 2003.

5.2. QuikSCAT Algorithm for Retrieval of Snow Accumulation

[21] Our algorithm exploits the inverse relationship between backscatter and snow accumulation. The fundamental physics behind the linear relationship between backscatter in dB (not in the linear domain) and snow accumulation is the exponential function of backscatter attenuation due to snow cover depth. Consider the scattering configuration in Figure 7 depicting snow accumulation with a depth d from the snow surface to the ice layer formation created during the previous melt time block. The total backscatter is dominated by electromagnetic wave scattering (represented by long arrows in Figure 7) from large scatterers in the ice layer, with negligible scattering (denoted with small arrows in Figure 7) from small snow grains and snow surface scattering at large incidence angles (46° for H polarization and 54° for V polarization). In this case, the backscatter is approximated by:

$$\sigma_0 = \sigma_I \cdot \exp(-\kappa \cdot d) \tag{1}$$

where κ is the two-way attenuation (including the cosine factor of the incidence wave field) in snow, σ_I is the initial direct scattering from the ice layer, and d is the snow accumulation depth [*Nghiem et al.*, 1990]. Taking the base-10 logarithm and multiplying both sides of the above equation by 10, we have the result (in dB):

$$\sigma_0 = \sigma_I - \alpha \cdot d \quad \text{for } \alpha = 10 \cdot \kappa \cdot \log_{10} e \tag{2}$$

This result indicates the linearity of backscatter in dB with the snow accumulation depth. To derive snow accumulation depth from QuikSCAT data, we take $d = (\sigma_I - \sigma_0)/\alpha$ where σ_0 is the current backscatter and σ_I is the initial backscatter at the beginning of the freezing season after the last melt in the preceding melt time block $\Delta\tau_m$.

[22] Theoretical models to calculate the attenuation coefficient α from the physical characteristics of snow under the renormalization method and the bilocal approximation (accounting for multiple electromagnetic wave interactions and

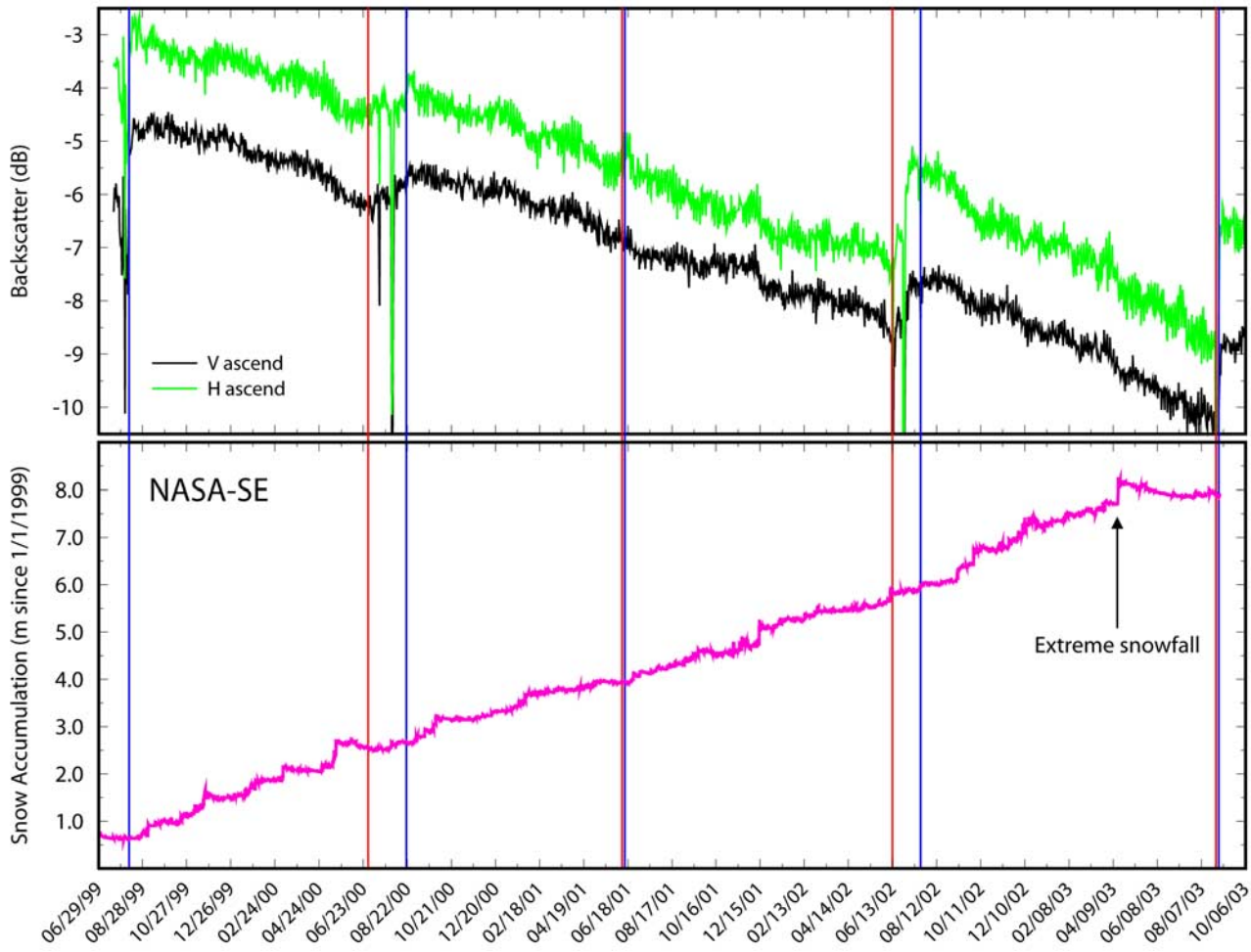

Figure 6. Backscatter and snow accumulation referenced from the snow level on 1 January 1999 at NASA-SE. The arrow indicates the date (15 April 2003) when an extreme snowfall occurred.

including both scattering and absorption losses in the attenuation) are developed and published in the literature [*Nghiem et al.*, 1990, 1993, 1995, 2001]. However, in situ snow height recordings from the GC-Net AWS offer a direct method to estimate α in the percolation zone of the Greenland ice sheet. The surface height change is recorded with two sonic height instruments at each AWS location. The recorded snow height change is the sum of snow accumulation minus sublimation and snow densification. Snow densification, caused by pressure and grain growth under freezing conditions, is on the order of a few centimeters over an annual cycle [*Zwally and Jun*, 2002] and has been neglected. The height change due to sublimation can be neglected since the rate is only 2% of the accumulation in the percolation region of the ice sheet [*Box and Steffen*, 2001]. Linear regression of AWS snow accumulation data at the NASA-SE location shows a very high correlation between σ_0 and d with the correlation coefficient (see Table 2) ranging from -0.874 to -0.941 for the four different freezing seasons from 1999 to 2003. Values of α are similar for all freezing seasons except for 1999–2000 when α is anomalously high and the correlation coefficient is its lowest (Table 2). The mean value of α is 0.905 for all freezing seasons from 1999 to 2003, with the exclusion of

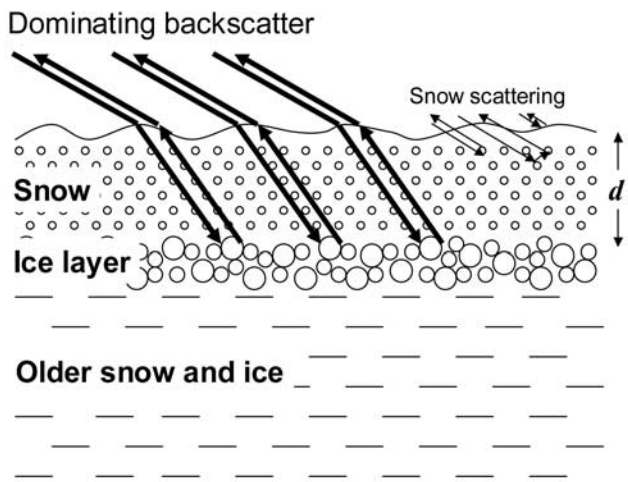

Figure 7. Scattering from a snow-covered ice layer.

Table 2. Results at NASA-SE and Comparison of Snow Accumulation Rate and Total Accumulation Measured by AWS and Derived From QuikSCAT Data[a]

	Freezing Season			
	1999–2000	2000–2001	2001–2002	2002–2003
Correlation coefficient	−0.874	−0.882	−0.909	−0.941
Attenuation α, dB/m	1.12	0.723	0.884	0.893
AWS accumulation rate, mm/day	6.2	4.4	4.9	7.3
QuikSCAT accumulation rate, mm/day	3.9	4.3	4.2	7.0
Mean deviation, %	22.8	2.2	7.7	2.1
AWS total accumulation, m	1.9	1.3	1.7	2.8
QuikSCAT total accumulation, m	1.4	1.5	2.0	3.0
Mean deviation, %	15.2	7.1	8.1	3.4

[a]Results for 2002–2003 exclude the surface lowering effect after the 2003 extreme snowfall (dark green area in Figure 8).

the time period following the large snow fall event in spring 2003, which will be discussed later.

5.3. Snow Accumulation Results for Multiple Annual Cycles at NASA-SE

[23] Using values of α, we derive the snow accumulation depth over the multiyear record in the NASA-SE area. The results are presented in Figure 8 for snow accumulation depths derived from QuikSCAT data with an individual α value obtained for each freezing season (indigo curves) and with the mean α value of 0.905 dB/m for all freezing seasons (black curves). The comparison of QuikSCAT results with measured accumulation at NASA-SE (Figure 8) shows a good agreement for all seasons (1999–2003). We estimate both the annual snow accumulation total and the snow accumulation rate from QuikSCAT data. Annual results are presented in Table 2 with comparisons to in situ measurements at NASA-SE. Overall, QuikSCAT and AWS values agree well with mean deviations around 2% to 8% (except for the 1999–2000 freezing season to be discussed below).

[24] The 1999–2003 data record at the NASA-SE AWS shows several severe snowfall events characterized by sharp increases in the curve of measured snow accumulation (Figure 6). Among these events, the April 2003 snowfall is the most recent and is one of the most anomalous in the NASA-SE record. The April 2003 snowfall extreme and the anomalous snow accumulation rate in 2002–2003 have attracted considerable interest and are addressed in a number of recent publications [*Box et al.*, 2005; *Nghiem et al.*, 2005; *Krabill et al.*, 2004; *Nghiem*, 2004]. Interestingly, QuikSCAT results capture the extreme snowfall in mid-April 2003 (Figure 8). Furthermore, snow accumulation derived from QuikSCAT data detects the anomalous accumulation rate and total snow accumulation during most of the 2002–2003 season at NASA-SE, which are significantly larger than those in all of the previous years (1999–2002) as shown in Figure 8 and in Table 2. The agreement between QuikSCAT and AWS results is better than 10% in most cases (Table 2) although QuikSCAT data are integrated over a 25 km × 25 km footprint while AWS data are point measurements. To indicate the spatial variability in AWS

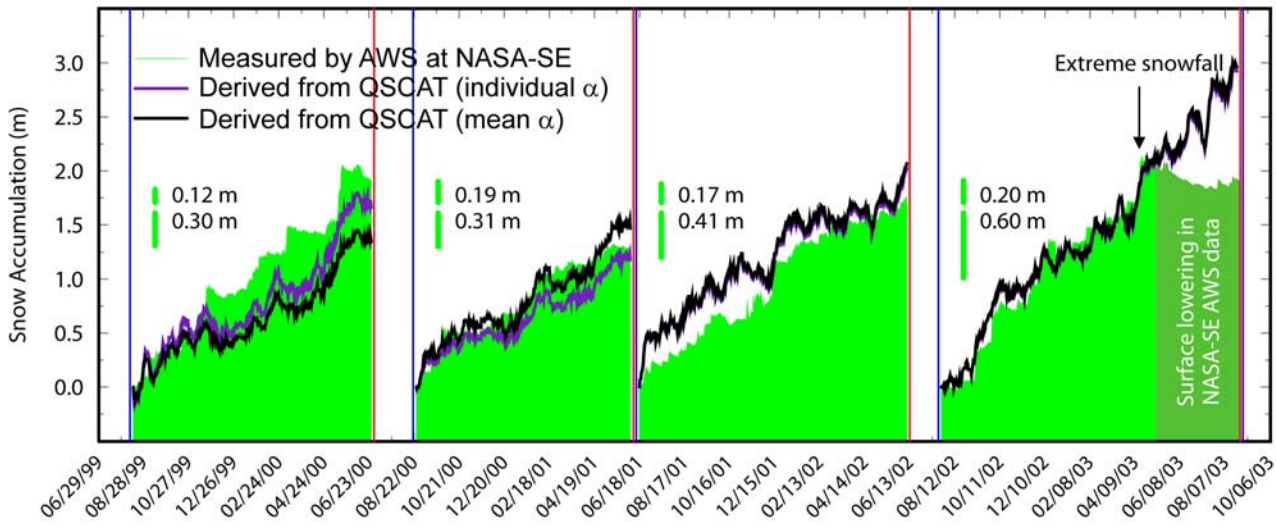

Figure 8. Snow accumulation at NASA-SE measured by AWS and derived from QuikSCAT data. The top number and the vertical green bar next to it represent the root mean square difference between two snow height sensors (separated by about 5 m) at the NASA-SE AWS; the bottom number and the adjacent green bar denote the maximum difference for each freezing season. QuikSCAT results capture the extreme snowfall in April 2003 indicated by the arrow. After the snow event, AWS data show surface lowering (dark green area) possibly due to wind erosion of this new snow layer at the NASA-SE site.

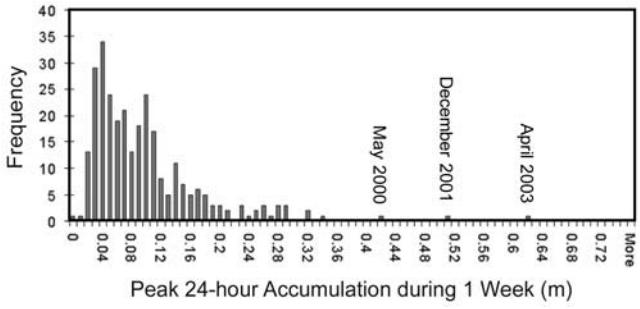

Figure 9. Frequency of peak accumulation in 24 hours during any given week derived from NASA-SE AWS data for 1999–2003. The snow event in April 2003 shows up as the most extreme on record.

point measurements, we present (Figure 8) root mean square and maximum values of the difference in snow height measurements recorded at NASA-SE by the two sonic sensors separated by approximately 5 meters in horizontal distance.

[25] For the 1999–2000 freezing season, the measured versus derived accumulation values agree fairly well during the first third of the freezing season; however, there can be more than 20% mean deviation during the remainder of the season. A closer examination of the 1999–2000 AWS data reveals a number of peculiar events during which snow accumulation discontinuously jumped sharply to a significantly higher level in the later part of the 1999–2000 season. This could be the result of transient or localized conditions such as heavy snowfall or strong snowdrift at NASA-SE for this particular time period, which were not representative of the 25-km scale seen by QuikSCAT.

[26] In 2003, AWS data at NASA-SE show a surface lowering effect (dark green area in Figure 8) after the extreme snowfall in mid-April, which deposited more than 0.5 m of snow in a day. This large snow precipitation volume is equivalent to the snow amount accumulated over 3 months based on the average accumulation rate of 5.2 mm/day for 1999–2002. This snowfall event exceeded all previously measured events since the installation of the AWS in the spring of 1998. A frequency analysis of peak accumulation in 24 hours for any given week of the year from 1999 to 2003 using AWS data at NASA-SE confirms that the snow event in April 2003 is the most anomalous compared to several extreme snow events on the record shown in Figure 9.

[27] Note that the 2003 extreme snowfall occurred under temperatures well below freezing (Figure 2), and the wind erosion of this new snow layer was an important factor in the surface lowering effect at the specific NASA-SE location. The redistribution of low-density snow is common on the ice sheet, in particular in regions with undulating surface topography (wavelength $\sim$ 5–10 km, height $\sim$ 30–50 m) as found around the NASA-SE location. This postulation is based on a case study along the western slope of the Greenland ice sheet near Crawford AWS (Figure 1). Two automatic weather stations from the GC-Net, separated by 6 km, were operating at or near Crawford. One AWS is situated atop a crest of the undulating surface and has been operational since May 1995 providing accumulation data along with a suite of climatological measurements (temperature, pressure, humidity, wind speed and direction, etc.) every hour. The second AWS is located 6 km (half a wavelength) upslope and is situated in the bottom of a trough. The latter AWS, which is identically equipped, has been operational from May 1997 to 2001. The acoustic height measurements from these two sites revealed a 37% difference in surface height change due to redistribution of low-density snow. This process explains low-density snow redistribution after an extreme snow event, such as the April 2003 event at the NASA-SE AWS. Hence we exclude the lowering effect in our QuikSCAT analysis, which covers a 25-km scale.

[28] An important observation (Figure 8) is that there is only a minor difference between the snow accumulation results derived from individual and mean values of α. This suggests that the snow accumulation algorithm can be significantly simplified by using the mean α. Similar analyses at NASA-U on the western slope of Greenland, where there is significantly less snow accumulation as compared to that at NASA-SE, show that the mean α works equally well. These analyses suggest that the mean α is applicable at different locations in the Greenland percolation zone and during different years.

5.4. Semiannual Snow Accumulation Maps From QuikSCAT Data

[29] On the basis of the above we propose the use of the mean α in this initial algorithm development for snow accumulation mapping over the percolation zone. As an example, we use the mean α to derive large-scale snow accumulation from weekly averaged QuikSCAT cell data at the horizontal polarization for the period between 7 October 2001 and 23 March 2002 (approximately half a year) for the percolation region of the Greenland ice sheet (Figure 10). We choose these fixed dates to obtain consistent results over Greenland, ensuring that no melt occurred and thus avoiding unstable backscatter values. The map in Figure 10 for the 2001–2002 freezing season shows more accumulation in the southeast side of Greenland, where NASA-SE is located, and little accumulation in the central western region, where NASA-U is located (Figure 1). The results agree with the typical accumulation at NASA-SE and NASA-U presented above. Furthermore, the overall pattern is consistent with the snow accumulation climatology of Greenland [*Benson*, 1962; *Ohmura and Reeh*, 1991; *Bales et al.*, 2001].

[30] To detect the extent of the anomalous snow accumulation in southeastern Greenland for the 2002–2003 freezing season, we derived the snow accumulation map for the same period between 7 October 2002 and 23 March 2003 (Figure 11). There was no melt during this time period; however, in April 2003, the first melt had occurred at several locations such as JAR 3, Dye-2, Saddle, and KULU (see locations in Figure 1). Because the fixed date approach is applied to the time period before April, the mid-April 2003 extreme snow event is not included in the result in Figure 11. Even with the exclusion of the extreme snowfall, the map in Figure 11 reveals a large region of high snow accumulation along the southeast region of the Greenland ice sheet. In this region, there were areas containing more than 3 m of snow accumulation over just 5.5 months. Such

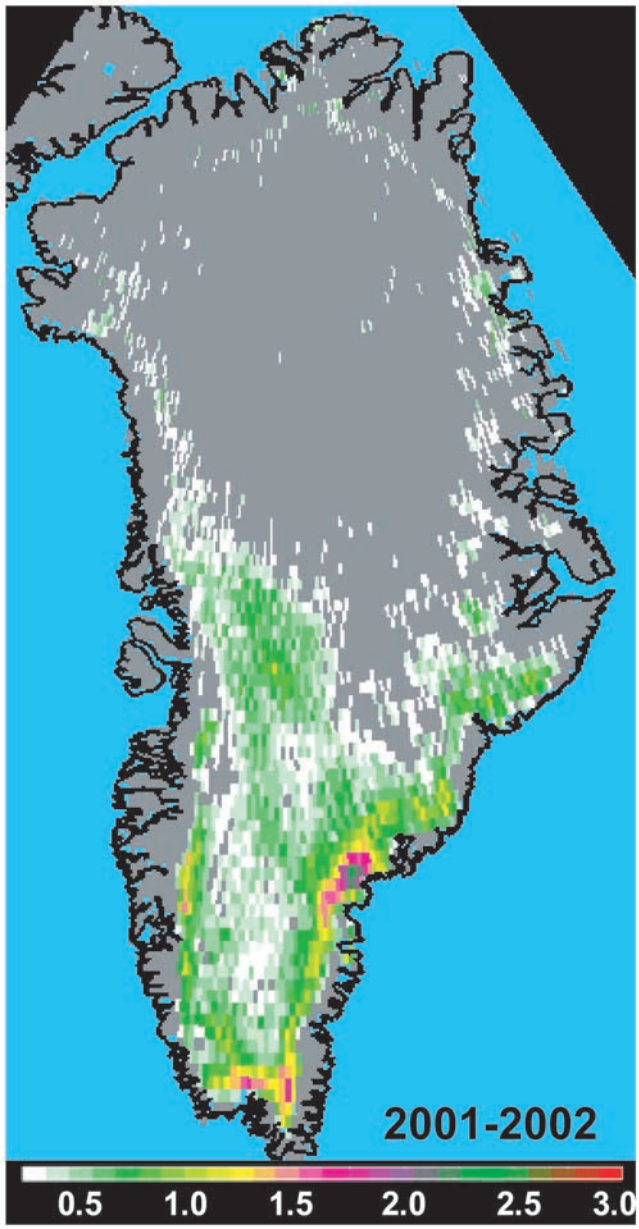

Figure 10. Snow accumulation in terms of snow depth (color scale unit in meters) over Greenland for the time span from 7 October 2001 to 23 March 2002 (5.5-month time span). Snow accumulation is seen largely over the Greenland percolation zone.

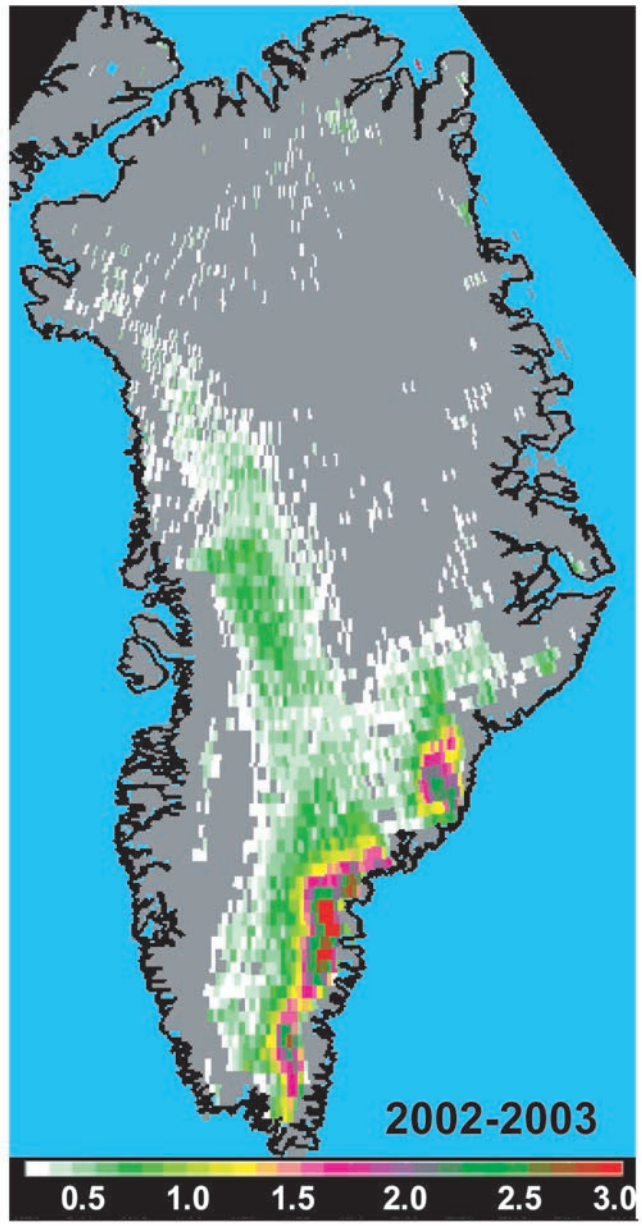

Figure 11. Snow accumulation in terms of snow depth (color scale unit in meters) over Greenland for the time span from 7 October 2002 to 23 March 2003 (5.5 months). Snow accumulation in the 2002–2003 freezing season is significantly higher over the southeast region and lower over the southwest region compared to the 2001–2002 freezing season.

an accumulation rate was well above the values for the previous freezing season (2001–2002) for the same region. Thus the snow accumulation anomaly occurred on the seasonal timescale during 2002–2003 as observed in the semiannual snow accumulation map (Figure 11), even excluding the single anomalous snow event in April 2003. However, there were also regions with reduced accumulation rates during the 2002–2003 freezing season, particularly in the southwest of the ice sheet.

[31] We caution that results shown in Figures 10 and 11 do not represent the complete total snow accumulation over the given freezing season because we used the fixed date approach in this initial snow accumulation algorithm. To account for the total accumulation during a full freezing season will necessitate the use of time domain analysis that treats each pixel with the whole time series record of QuikSCAT data to accurately determine the melt timing at each pixel over the Greenland ice sheet. This timing is different for different pixels at different locations in Greenland. Then, the full time span of the complete freezing season can be derived and the total seasonal snow accumulation can be obtained at every pixel. We will implement

this advanced algorithm to obtain the full accumulation results in the future.

6. Conclusions

[32] Greenland Climate Network measurements provide crucial in situ data to facilitate the interpretation of QuikSCAT backscatter signatures for the development of new algorithms to map ice layer formation extent and snow accumulation. Ice scatterers formed by the percolation of melting water that refreezes in the firn layer increase the backscatter. This effect allows QuikSCAT data to be used to detect and map the extent of ice layer formation. Results for year 2002 show an extensive ice layer formation consistent with the record melt area extent during the same year. In a freezing season, snow accumulation in the percolation zone attenuates QuikSCAT backscatter resulting in a linear backscatter decrease (in dB). The attenuation effect enables the retrieval of snow accumulation depth using QuikSCAT data. Snow accumulation results from QuikSCAT compare well, within the measurement uncertainties, with snow height data at the NASA-SE station of the Greenland Climate Network (excluding the surface lowering effect after the extreme snow event in mid-April 2003), where snow accumulation during the 2002–2003 freezing season anomalously increased by a factor of 2 compared to the accumulation in previous freezing seasons. QuikSCAT results for snow accumulation were capable of detecting and capturing the 2003 extreme snowfall.

[33] Large-scale snow accumulation maps for a period of 5.5 months in two consecutive freezing seasons, 2001–2002 and 2002–2003, reveal an extensive snow accumulation anomaly on the southeast side of the Greenland ice sheet in 2002–2003 and a slight decrease in accumulation on the southwest side in the same season as compared to the 2001–2002 season. These results demonstrate the complexity of seasonal and interannual patterns and changes in ice layer formation and snow accumulation that directly impact the overall Greenland ice mass balance. Note that the snow accumulation regions presented in Figures 10 and 11 are largely located within the percolation zone. From the scattering physics illustrated in Figure 7, the basis for this approach for deriving snow accumulation is the strong backscatter from large scatterers in an ice layer formed by melt metamorphosis in the firn layer. The ice layer can form during the preceding melt time block or even from years further in the past as long as the snow cover is not too thick to mask out the backscatter signature of the ice layer formation. In the percolation zone, melt events release water that refreezes in the cold firn layers, and thus this approach is applicable.

[34] For areas where snow has accumulated for a long time without significant melt to create large ice scatterers or an area where no melt occurs like the dry snow zone, this method is not appropriate. For the dry snow zone, the use of C-band radar to map snow accumulation has been demonstrated [*Munk et al.*, 2003], and thus Ku-band and C-band radar data form a complimentary data combination for snow accumulation measurements over most of the Greenland ice sheet. However, none of the methods described above can be used to derive accumulation rates in the ablation region.

[35] Advanced algorithms will be developed to fully map the extent of ice layer formation and total annual snow accumulation in the percolation zone of the Greenland ice sheet in the long term as satellite scatterometer data acquisition continues on into a decadal timescale. Furthermore, anomalous snow accumulation patterns such as those observed in the 2002–2003 freezing season can cross-verify results obtained by ICESat (Ice, Cloud, and land Elevation Satellite Mission) or by GRACE (Gravity Recovery and Climate Experiment Mission). Future advanced scatterometer measurements with a high resolution (1 to 5 km) would continue the long-term scatterometer time series data, and account for high spatial gradient patterns of snow accumulation in regions with undulating surface topography and in the steep topographic regime around the Greenland ice sheet.

[36] **Acknowledgments.** The research carried out at the Jet Propulsion Laboratory (JPL), California Institute of Technology, was supported by the National Aeronautics and Space Administration (NASA). The research carried out at the Cooperative Institute for Research in Environmental Sciences, University of Colorado, was also supported by the NASA Cryospheric Sciences Research Program. We thank G. Flowers for her careful review of this paper.

References

Bales, R. C., J. R. McConnell, E. Mosley-Thompson, and B. Csatho (2001), Accumulation over the Greenland ice sheet from historical and recent records, *J. Geophys. Res.*, *106*(D24), 33,813–33,825.

Benson, C. S. (1962), Stratigraphic studies in the snow and firn on the Greenland ice sheet, *Res. Rep. 70*, Snow, Ice, and Permafrost Res. Estab., U.S. Army Corps of Eng., Hanover, N. H.

Box, J. E., and K. Steffen (2001), Sublimation on the Greenland ice sheet from automated weather station observations, *J. Geophys. Res.*, *106*(D24), 33,965–33,982.

Box, J., L. Yang, J. Rogers, D. Bromwich, L.-S. Bai, K. Steffen, J. Stroeve, and S.-H. Wang (2005), Extreme precipitation events over Greenland: Consequences to ice sheet mass balance, paper presented at 8th Conference on Polar Meteorology and Oceanography, Am. Meteorol. Soc., San Diego, Calif.

Braithwaite, R. J., M. Laternser, and T. W. Pfeffer (1994), Variations of near-surface firn density in the lower accumulation area of the Greenland ice sheet, Pakitsoq, West Greenland, *J. Glaciol.*, *40*(136), 477–485.

Davis, C. H., C. A. Kluever, and B. J. Haines (1998), Elevation change of the southern Greenland ice sheet, *Science*, *279*, 2086–2088.

Drinkwater, M. R., D. G. Long, and A. W. Bingham (2001), Greenland snow accumulation estimates from satellite radar scatteromter data, *J. Geophys. Res.*, *106*(D24), 33,935–33,950.

Jezek, K. C., M. R. Drinkwater, J. P. Crawford, and R. Kwok (1993), Analysis of synthetic aperture radar data collected over the southwestern Greenland ice sheet, *J. Glaciol.*, *39*(131), 119–132.

Krabill, W., et al. (2004), Greenland ice sheet: Increased coastal thinning, *Geophys. Res. Lett.*, *31*, L24402, doi:10.1029/2004GL021533.

McConnell, J. R., R. J. Arthern, E. Mosley-Thompson, C. H. Davis, R. C. Bales, R. Thomas, J. F. Burkhart, and J. D. Kyne (2000), Changes in Greenland ice sheet elevation attributed primarily to snow accumulation variability, *Nature*, *406*, 877–879.

Munk, J., K. C. Jezek, R. R. Foster, and S. P. Gogineni (2003), An accumulation map for the Greenland dry-snow facies derived from spaceborne radar, *J. Geophys. Res.*, *108*(D9), 4280, doi:10.1029/2002JD002481.

Nghiem, S. V. (2004), Observations of Arctic environmental change, paper presented at International Geoscience Remote Sensing Symposium, Geosci. and Remote Sens. Soc., Anchorage, Alaska.

Nghiem, S. V., M. Borgeaud, J. A. Kong, and R. T. Shin (1990), Polarimetric remote sensing of geophysical media with layer random medium model, in *Progress in Electromagnetics Research*, vol. 3, chap. 1, pp. 1–73, Elsevier, New York.

Nghiem, S. V., R. Kwok, J. A. Kong, and R. T. Shin (1993), A model with ellipsoidal scatterers for polarimetric remote sensing of anisotropic layered media, *Radio Sci.*, *28*(5), 687–703.

Nghiem, S. V., R. Kwok, S. H. Yueh, J. A. Kong, M. A. Tassoudji, C. C. Hsu, and R. T. Shin (1995), Polarimetric scattering from layered media with multiple species of scatterers, *Radio Sci.*, *30*(4), 835–852.

Nghiem, S. V., K. Steffen, R. Kwok, and W. Y. Tsai (2001), Detection of snowmelt regions on the Greenland ice sheet using diurnal backscatter change, *J. Glaciol.*, *47*(159), 539–547.

Nghiem, S. V., K. Steffen, R. Huff, and G. Neumann (2005), Anomalous snow accumulation over the southeast region of the Greenland ice sheet during 2002–2003 snow season, paper presented at 8th Conference on Polar Meteorology and Oceanography, Am. Meteorol. Soc., San Diego, Calif.

Ohmura, A., and N. Reeh (1991), New precipitation and accumulation maps for Greenland, *J. Glaciol.*, *37*(125), 140–148.

Smith, L. C., Y. Sheng, R. R. Forster, K. Steffen, K. E. Frey, and D. E. Alsdorf (2003), Melting of small Arctic ice caps observed from ERS scatterometer time series, *Geophys. Res. Lett.*, *30*(20), 2034, doi:10.1029/2003GL017641.

Steffen, K., and J. E. Box (2001), Surface climatology of the Greenland ice sheet: Greenland climate network 1995–1999, *J. Geophys. Res.*, *106*(D24), 33,065–33,982.

Steffen, K., S. V. Nghiem, R. Huff, and G. Neumann (2004), The melt anomaly of 2002 on the Greenland ice sheet from active and passive microwave satellite observations, *Geophys. Res. Lett.*, *31*, L20402, doi:10.1029/2004GL020444.

Sturm, M., D. K. Perovich, and M. Serreze (2003), Meltdown in the North, *Sci. Am.*, *288*(4), 60–67.

Thomas, R. H., W. Abdalati, E. Frederick, W. B. Krabill, S. Manizade, and K. Steffen (2003), Investigation of surface melting and dynamic thinning on Jakobshavn Isbrea, Greenland, *J. Glaciol.*, *49*(165), 231–239.

Tsai, W.-Y., S. V. Nghiem, J. N. Huddleston, M. W. Spencer, B. W. Stiles, and R. D. West (2000), Polarimetric scatterometry: A promising technique for improving ocean surface wind measurements, *IEEE Trans. Geosci. Remote Sens.*, *38*(4), 1903–1921.

Wismann, V. (2000), Monitoring of seasonal snowmelt in Greenland with ERS scatterometer data, *IEEE Trans. Geosci. Remote Sens.*, *38*(4), 1821–1826.

Zwally, H. J., and L. Jun (2002), Seasonal and interannual variations of firn densification and ice sheet surface elevation at the Greenland summit, *J. Glaciol.*, *48*(1610), 199–207.

Zwally, H. J., A. C. Brenner, and J. P. DiMarzio (1998), Comment: Growth of the southern Greenland ice sheet, *Science*, *281*, 1251.

R. Huff and K. Steffen, Cooperative Institute for Research in Environmental Sciences, University of Colorado, Boulder, CO 80309, USA.

G. Neumann and S. V. Nghiem, JPL, MS 300-235, 4800 Oak Grove Drive, Pasadena, CA 91109, USA. (son.v.nghiem@jpl.nasa.gov)